ANTIMICROBIAL AGENTS AND CHEMOTHERAPY, May 2005, p. 1837–1843 Vol. 49, No. 5
0066-4804/05/$08.00+0 doi:10.1128/AAC.49.5.1837–1843.2005

Imidazole Antibiotics Inhibit the Nitric Oxide Dioxygenase Function of Microbial Flavohemoglobin

Ryan A. Helmick,[1] Arin E. Fletcher,[1] Anne M. Gardner,[1] Christopher R. Gessner,[1] Angela N. Hvitved,[2] Michael C. Gustin,[2] and Paul R. Gardner[1]*

Division of Critical Care Medicine, Cincinnati Children's Hospital Medical Center, and Department of Pediatrics, University of Cincinnati College of Medicine, Cincinnati, Ohio 45229,[1] and Department of Biochemistry and Cell Biology, Rice University, Houston, Texas 77251[2]

Received 24 July 2004/Returned for modification 25 October 2004/Accepted 24 January 2005

Flavohemoglobins metabolize nitric oxide (NO) to nitrate and protect bacteria and fungi from NO-mediated damage, growth inhibition, and killing by NO-releasing immune cells. Antimicrobial imidazoles were tested for their ability to coordinate flavohemoglobin and inhibit its NO dioxygenase (NOD) function. Miconazole, econazole, clotrimazole, and ketoconazole inhibited the NOD activity of *Escherichia coli* flavohemoglobin with apparent K_i values of 80, 550, 1,300, and 5,000 nM, respectively. *Saccharomyces cerevisiae*, *Candida albicans*, and *Alcaligenes eutrophus* enzymes exhibited similar sensitivities to imidazoles. Imidazoles coordinated the heme iron atom, impaired ferric heme reduction, produced uncompetitive inhibition with respect to O_2 and NO, and inhibited NO metabolism by yeasts and bacteria. Nevertheless, these imidazoles were not sufficiently selective to fully mimic the NO-dependent growth stasis seen with NOD-deficient mutants. The results demonstrate a mechanism for NOD inhibition by imidazoles and suggest a target for imidazole engineering.

Nitric oxide (NO) is released by macrophages and other immune cells to poison and help eliminate infectious microbes, parasites, and tumor cells (12, 27, 41). Diverse life forms protect against NO toxicity by expressing NO-metabolizing enzymes. NO dioxygenases (NODs) (EC 1.14.12.17) convert NO to NO_3^- (equation 1), while in some organisms NO reductases (NORs) (EC 1.7.99.7) reduce NO to N_2O (equation 2) (18, 39, 64). NODs utilize O_2 for NO detoxification, whereas NORs scavenge and detoxify NO under anaerobic conditions and supplement NOD under the microaerobic conditions found in infections (16–18, 20).

$$2\ NO + 2\ O_2 + NAD(P)H \rightarrow 2\ NO_3^- + NAD(P)^+ + H^+ \quad (1)$$

$$2\ NO + NADH + H^+ \rightarrow N_2O + NAD^+ + H_2O \quad (2)$$

Genomic microarrays of *Escherichia coli*, *Bacillus subtilis*, and *Pseudomonas aeruginosa* reveal NOD (*hmp*) and NOR gene transcription prominently induced by NO in vitro (37, 38). *Salmonella enterica* expresses NOD (*hmp*) and NOR (*norVW*) gene transcripts at high levels in infected macrophages, indicating roles in adaptation to macrophage NO (10). In addition, DNA microarrays of immune-resistant mucoid isolates of *P. aeruginosa* reveal NOD (*fhb*) and NOR (*norBC*) gene transcript levels elevated >50-fold, suggesting roles in the virulence of these *P. aeruginosa* strains (14). Moreover, NODs have been shown to prevent NO-mediated growth inhibition of bacteria, yeasts, and fungi (4, 7, 15, 20, 25, 26, 31, 36, 46, 55), decrease the susceptibility of *Salmonella* to killing by macrophages (51), and modestly increase the virulence of *Cryptococcus neoformans* and *Candida albicans* in systemic infections of mice (7, 55). NODs, NORs, and other microbial defense enzymes have thus emerged as attractive targets for antibiotic development (40). Agents that selectively target microbial defenses are expected to generate antibiotic-resistant mutants at reduced frequencies given the coordinate production of myriad antimicrobial toxins including NO, H_2O_2, HOCl, and O_2^- during the innate immune response and the multiple sites for toxin actions (12, 20).

The well-characterized flavohemoglobins (flavoHbs) and single domain hemoglobins (Hbs) with their associated reductases function as NODs in a variety of human and plant pathogens, including *E. coli*, *S. enterica* serovar Typhimurium, *C. albicans*, *C. neoformans*, *Klebsiella pneumonia*, *P. aeruginosa*, *Mycobacterium tuberculosis*, and *Erwinia chrysanthemi* (7, 13, 15, 20, 45, 46, 55), and genes encoding (flavo)Hbs are found in diverse microbes. In contrast, infectious microbes express one of three different types of NORs; however, not all organisms employ NORs for NO detoxification (18, 64).

Inhibitors that target the heme prosthetic group of (flavo)Hbs are attractive candidates for antibiotic development. Imidazoles bearing bulky aromatic substituents offer potential for selective and high-affinity inhibition of NOD function by coordinating the catalytic heme iron and "fitting" within the large hydrophobic distal heme pocket (11, 20, 28, 44). Imidazole coordinates the ferric iron atom of *E. coli* flavoHb with an equilibrium dissociation constant (K_d) of 333 μM (28), and imidazoles with bulky aromatic N-1 substituents bind and inhibit heme enzymes with similar hydrophobic pockets such as the cytochromes P450 Cyp51 (lanosterol 14α-demethylase) and Cyp121 (2, 35, 47, 63).

We have investigated the sensitivity of microbial NODs to imidazole derivatives at the enzymatic and cellular levels and propose a mechanism for NOD inhibition based on kinetic and spectroscopic data. Imidazole inhibition of microbial NOD is suggested as a strategy for increasing the antibiotic efficacy of immune system-derived NO.

* Corresponding author. Mailing address: Division of Critical Care Medicine, MLC7006, Children's Hospital Medical Center, 3333 Burnet Ave., Cincinnati, Ohio 45229. Phone: (513) 636-4885. Fax: (513) 636-4892. E-mail: paul.gardner@cchmc.org.

MATERIALS AND METHODS

Cells and plasmids. *Saccharomyces cerevisiae* strain BY4742 (*MATα his3Δ leu2Δ lys2Δ ura3Δ*) and its isogenic flavoHb-deficient derivative 15887 (*yhb1Δ*::KanMX) were from Research Genetics/Invitrogen. *C. albicans* strain RM1000 (*ura3Δ::imm*$^{434/ura3\Delta}$*::imm*^{434} *his1Δ::hisG/his1Δ::hisG*) was from Jesus Pla (Universidad Complutense de Madrid, Spain), and its isogenic flavoHb-deficient derivative *yhb1Δ/yhb1Δ* (*yhb1Δ::HIS1/yhb1Δ::dp1200*) was prepared as previously described (55). *Staphylococcus aureus* (ATCC 6538) was obtained from the American Type Culture Collection (Manassas, VA). Plasmid pEcHMP was constructed by subcloning the EcoRI-BamHI fragment of plasmid pAlter-*hmp* (16, 25) into pUC19 (61). Plasmid pCaYHB1 was constructed by inserting PCR-cloned DNA coding the full-length *C. albicans yhb1* gene into the NdeI-BamHI site of pANX. pANX is a derivative of pUC19 in which the 812-bp PvuII-SmaI promoter region of *E. coli hmp* has been inserted in the SmaI site of the polylinker of pUC19 in which the NdeI site has been removed. Insertion at the NdeI site of the *hmp* promoter creates a start methionine. All constructs were sequence verified.

Reagents. Bovine liver catalase (65,000 U/mg) and NADH were obtained from Roche Molecular Biochemicals (Indianapolis, IN). Hemin was obtained from Fluka (Basel, Switzerland). Samples of the *Alcaligenes eutrophus* (also known as *Ralstonia eutropha*) and *S. cerevisiae* flavoHbs were provided by Hao Zhu and Austen Riggs (University of Texas, Austin) (24). Gas cylinders, containing 1,200 ppm NO in ultrapure N_2, 99.993% O_2, 1.5% O_2 in ultrapure N_2, 99.998% N_2, and 99.999% argon, were obtained from Praxair (Bethlehem, PA). Miconazole (nitrate salt), econazole (nitrate salt), clotrimazole, ketoconazole, itraconazole, and all other reagents were purchased from Sigma-Aldrich Fine Chemicals (St. Louis, MO) unless otherwise indicated.

FlavoHb isolation and characterization. *E. coli* and *C. albicans* flavoHbs were expressed and purified from flavoHb-deficient *E. coli* AG103 cells (16), bearing the high-copy plasmids pEcHMP and pCaYHb1 and grown overnight in a nutrient-rich medium containing 89 mM potassium phosphate (pH 7.4), 24 g/liter Bacto yeast extract (Becton Dickinson, catalog no. 212750), 8 g/liter Bacto tryptone (Becton Dickinson, catalog no. 211705), 5 g/liter glycerol, 10 mM sodium nitrate, 260 U/ml catalase, 0.2 μM hemin, and 150 μg/ml ampicillin. Cultures were grown in 1-liter flasks at a culture-headspace volume ratio of 9:1 and were agitated in a gyrorotary shaker at 100 rpm. Cells were harvested, and flavoHbs were isolated as previously described (19). FlavoHbs were partly deficient in heme and FAD (flavin adenine dinucleotide) and were reconstituted by slowly adding a slight excess of hemin relative to heme-deficient sites (≤0.5 mM) in the presence of 10 mM dithiothreitol, 1 mM EDTA, and 2,000 U/ml catalase in 1.5 ml of 50 mM Tris-Cl buffer, pH 8.0, adding ~1 mg dithionite, and incubating at 37°C for 60 min. Reductants and free hemin were removed by gel filtration on a Superdex 75 column in N_2-scrubbed elution buffer containing 50 mM Tris-Cl, pH 8.0, 1 mM EDTA, and 32 U/ml catalase. Reconstituted *E. coli* and *C. albicans* flavoHbs contained 69 and 85% heme, respectively. FlavoHbs were reconstituted with FAD by adding stoichiometric amounts of FAD.

Heme and FAD were assayed as previously described (19), and protein was assayed using the Lowry method (32) with bovine serum albumin (fraction V) as the standard using a 280-nm absorbance value of 0.627 for 1 mg/ml (43). FlavoHb purity was estimated to be >95% by sodium dodecyl sulfate-polyacrylamide gel electrophoresis.

NOD activity assays. NOD activity was assayed amperometrically in 100 mM sodium phosphate buffer, pH 7.0, containing 0.3 mM EDTA, 100 μM NADH, and 1 μM FAD at 37°C, and NO and O_2 concentrations were varied as previously described (19, 23). Inhibition by imidazoles was measured at 200 μM O_2 and 1 μM NO unless otherwise indicated. Specific activities of the *E. coli*, *A. eutrophus*, *S. cerevisiae*, and *C. albicans* flavoHbs at 200 μM O_2 and 1 μM NO were 185, 90, 105, and 17 NO heme^{-1} s^{-1}, respectively. NO metabolism by cells was measured at 37°C in phosphate-buffered medium containing glucose and inhibitors of protein synthesis (18, 23, 55).

Spectral analysis. FlavoHbs were scanned at 20°C in anaerobic 100 mM sodium phosphate, pH 7.0, buffer containing 0.3 mM EDTA in rubber septum-sealed quartz cuvettes scrubbed with argon to remove O_2. Residual O_2 was removed by adding 8 U/ml glucose oxidase, 5 mM glucose, and 260 U/ml catalase to buffers. All other experimental details are provided in the figure legends.

Culture growth and NO exposures. *E. coli* AG103 pEcHMP was grown as described above to an A_{550} of 2.0, and cells were harvested as previously described (22). *S. cerevisiae* was grown at 30°C with aeration in yeast peptone dextrose (YPD) medium containing 10 g/liter Bacto yeast extract (Becton Dickinson, catalog no. 212750), 20 g/liter Bacto peptone (Becton Dickinson, catalog no. 211677), and 20 g/liter glucose (55). *S. cerevisiae* was grown to early log phase (A_{600} = 0.6), harvested, and assayed for NO metabolism. *C. albicans* strain RM1000 was grown at 37°C in YPD medium supplemented with 50 mg/liter uridine, 20 mg/liter adenine, 100 mg/liter leucine, and 20 mg/liter tryptophan to ensure maximal growth and NOD activity induction. At an A_{600} of 0.25, RM1000 cultures were exposed to 960 ppm NO in an atmosphere containing 21% O_2 for 60 min (55). *S. aureus* cultures were grown at 37°C with aeration in phosphate-buffered Luria broth (22) to an A_{550} of 0.05 and exposed to 960 ppm NO in an atmosphere containing 21% O_2 for 120 min. Cultures were quickly chilled on ice to inhibit growth and protein synthesis, harvested, washed, and assayed for NO metabolism (22).

For growth and viability experiments, *S. cerevisiae* strains were grown at 30°C in YPD medium under an atmosphere containing 21% O_2 balanced with N_2 (220 μM O_2 in solution). *S. cerevisiae* cultures were initiated from overnight cultures with an initial A_{600} of 0.06. Dimethyl sulfoxide (DMSO) was added at 0.01% (vol/vol) as the solvent for miconazole. *C. albicans* strains were grown at 37°C in a modified YPD medium containing 5 mM glucose under an atmosphere containing 1.05% O_2 balanced with N_2 (10 μM O_2 in solution) to better mimic the physiological conditions of tissue infections. Cultures were initiated from overnight cultures with an initial A_{600} of 0.04. After 30 min of initial growth, cultures were exposed to 160 ppm NO with or without 5 μM econazole. DMSO was added to 0.01% (vol/vol) as the solvent for econazole. Cell density was measured by plating, colony counting, and optical density measurements (21, 55).

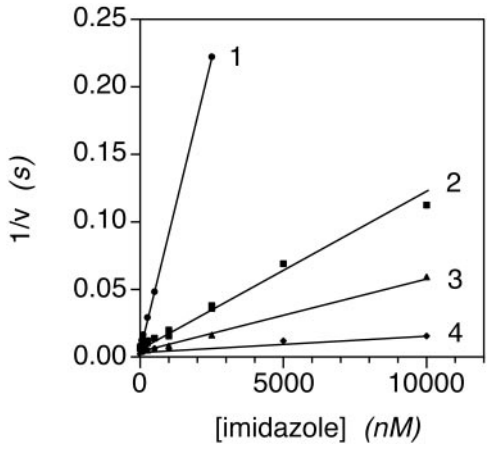

FIG. 1. Inhibition of *E. coli* NOD activity by imidazoles. NOD activity of *E. coli* flavoHb was assayed at the indicated concentrations of miconazole (line 1), econazole (line 2), clotrimazole (line 3), or ketoconazole (line 4). DMSO (lines 1–3) and methanol (line 4) were present at a final concentration of 0.1% (vol/vol).

RESULTS

Imidazoles inhibit microbial NODs. Antimicrobial imidazoles were tested for their ability to inhibit the NOD activity of purified flavoHbs. As shown for the *E. coli* NOD activity (Fig. 1), a linear relationship is observed for 1/*v* versus [imidazole], suggesting a reversible mechanism involving imidazole binding. Miconazole, econazole, clotrimazole, and ketoconazole inhibited *E. coli* NOD with apparent K_i values of 80, 550, 1,300, and 5,000 nM, respectively. *A. eutrophus*, *S. cerevisiae*, and *C. albicans* NOD activities showed similar inhibition kinetics with the exception of the *A. eutrophus* enzyme, which showed biphasic inhibition (data not shown). Biphasic inhibition may be due to partial retention of lipids in the hydrophobic distal heme pocket (44) or the existence of multiple conformational states. Apparent K_i values for the bacterial and *S. cerevisiae* enzymes reveal an order of potency: miconazole > econazole > clotrimazole > ketoconazole (Table 1). For the *C. albicans* enzyme, econazole was ~3-fold more effective than miconazole.

TABLE 1. Inhibition of the NOD activity of flavoHbs by imidazoles

Imidazole[a]	Apparent K_i (nM)			
	E. coli	*A. eutrophus*[b]	*S. cerevisiae*	*C. albicans*
Miconazole	80	5 (~70), 650 (~30)	12,000	700
Econazole	550	100 (~70), 2,000 (~30)	30,000	225
Clotrimazole	1,300	200 (~93), 5,000 (~7)	50,000	650
Ketoconazole	5,000	700 (~75), 25,000 (~25)	>100,000	12,500

[a] The solvents DMSO (miconazole, econazole, and clotrimazole) and methanol (ketoconazole) were present at a final concentration of 0.1% (vol/vol) and did not affect the activity.

[b] K_i values are estimated from biphasic plots of $1/v$ versus [imidazole]. The fraction inhibited for each phase is given in parentheses as a percentage of the total activity.

In comparison, the potent lanosterol 14α-demethylase inhibitor and antifungal agent itraconazole (6, 58), bearing a triazole and bulky substituent more similar in structure to that of ketoconazole than the other imidazoles (structures reviewed in reference 58), showed a weaker inhibition more similar to that of ketoconazole. At 2 μM, itraconazole inhibited *C. albicans* and *E. coli* NOD activities by 6% and 27%, respectively.

Inhibition by miconazole was uncompetitive with respect to O_2 and NO, as demonstrated by the parallel lines produced for $1/v$ versus $1/[O_2]$ (Fig. 2A) and $1/v$ versus $1/[NO]$ (Fig. 2B) with various concentrations of miconazole. It should be noted that high [NO] inhibited the enzyme by competing with O_2 for ferrous heme (19, 24) and that NO inhibition was augmented by miconazole (Fig. 2B).

Imidazoles bind oxidized and reduced flavoHb. Imidazoles were examined spectroscopically for their ability to coordinate the iron atom in *E. coli* flavoHb. Miconazole caused a 10-nm red shift of the Soret band (Table 2) and appearance of a strong β-band absorbance at 537 nm with a weak shoulder at 570 nm (data not shown), indicating imidazole nitrogen coordination to produce a hexacoordinate low-spin heme iron. Miconazole also coordinated ferrous heme iron as revealed by a 6-nm blue shift and enhancement of the Soret band and by the appearance of distinct β and α bands at 530 and 560 nm, respectively. Econazole, clotrimazole, and ketoconazole produced similar spectral changes (Table 2), indicating limited interference of N-1 substituents with heme iron coordination.

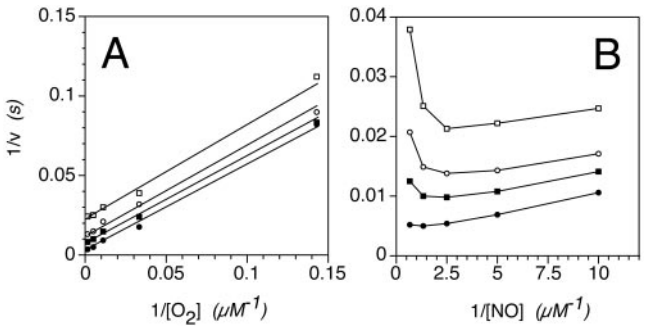

FIG. 2. NOD activity of *E. coli* flavoHb with various miconazole, O_2, and NO concentrations. NOD activity was assayed with various concentrations of O_2 and 0.75 μM NO (A) or with various concentrations of NO and 200 μM O_2 (B) in the presence of 0 μM (●), 0.1 μM (■), 0.25 μM (○), or 0.5 μM (□) miconazole. DMSO was present at a final concentration of 0.1% (vol/vol).

TABLE 2. Absorption maxima and extinction coefficients of *E. coli* flavoHb-imidazole complexes

FlavoHb complex	Soret maximum (λ) (nm [mM^{-1} cm^{-1}])[a]	Visible maxima (λ) (nm [mM^{-1} cm^{-1}])[a]
Fe(III)	403 (88.6)	460 (23.0), 628 (2.51)
Fe(II)	433 (58.4)	556 (6.90)
$Fe(II)O_2$	415 (117)	545 (14.1), 579 (6.89)
Fe(III)-miconazole	413 (103)	460 (25.7), 537 (9.26)
Fe(III)-econazole	414 (106)	460 (24.1), 537 (9.48)
Fe(III)-clotrimazole	414 (102)	460 (25.6), 537 (8.60)
Fe(III)-ketoconazole	414 (114)	460 (29.2), 537 (10.4)
Fe(II)-miconazole	427 (120)	530 (9.93), 560 (18.8)
Fe(II)-econazole	426 (114)	530 (9.53), 559 (16.3)
Fe(II)-clotrimazole	422 (89.7)	531 (9.08), 556 (10.4)
Fe(II)-ketoconazole	425 (113)	525 (8.76), 555 (14.0)

[a] Extinction coefficients are relative to the heme content of flavoHb.

Only minor differences in α- and β-band maxima of the ferrous complexes were observed with ketoconazole showing the largest effects.

Miconazole showed rapid, and near stoichiometric, coordination to flavoHb-Fe(III) (Fig. 3A). In contrast, miconazole associated weakly with the NADH-reduced ferrous form as evidenced by relatively slow coordination (data not shown) and substoichiometric formation of the Fe(II)-miconazole complex (Fig. 3B).

Imidazole binding impedes NADH-mediated reduction of heme and FAD. NOD function requires reduction of the ferric heme in the globin domain of flavoHb via an electron shuttle from free NADH to bound FAD to the heme (19, 20). Coordination of miconazole to the ferric heme iron inhibited heme and FAD reduction as evidenced by the slower rate of transition from the ferric to ferrous state with miconazole coordination (Fig. 4, compare panel B with panel A). A marked decrease in the rate of red shift and hypochromicity of the Soret band was observed during reduction of the ferric-miconazole

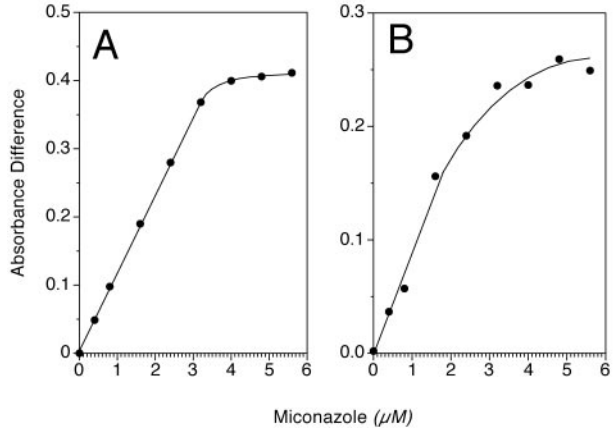

FIG. 3. Titration of oxidized and reduced flavoHb with miconazole. (A) Miconazole was added to *E. coli* flavoHb-Fe(III) (4.0 μM heme), and coordination was followed by measuring the absorbance differences for the maximum (417 nm) and minimum (382 nm) of difference spectra of the miconazole complex and free enzyme. (B) Miconazole was added to NADH-reduced flavoHb-Fe(II) (4.0 μM heme) under anaerobic conditions. Samples were incubated for 5 min to allow coordination, difference spectra were recorded, and the absorbance difference for the peak (412 nm) and trough (437 nm) were measured.

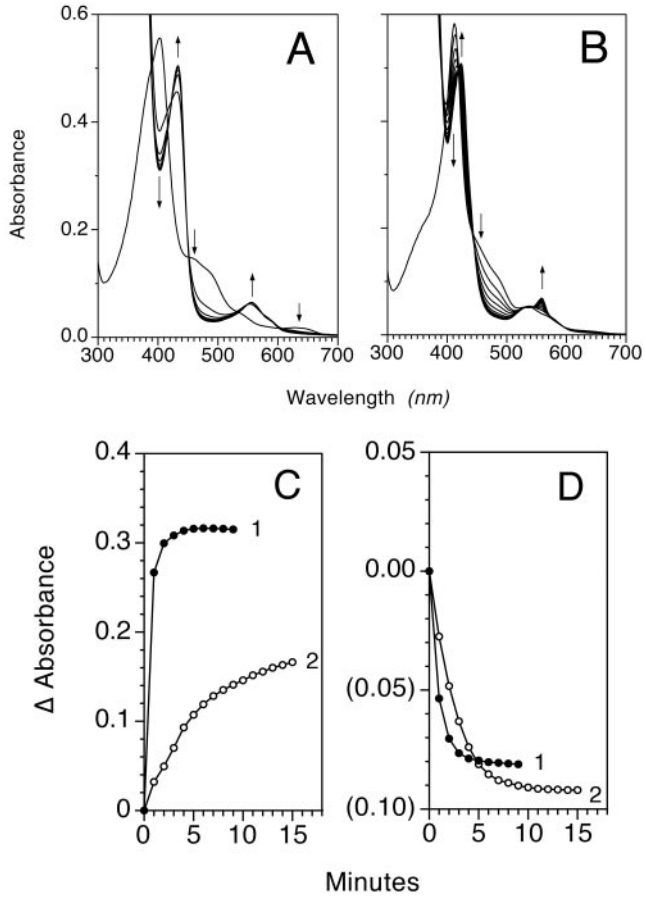

FIG. 4. NADH reduction of the flavoHb-Fe(III)-miconazole complex. (A) Spectra of *E. coli* flavoHb (6.0 μM heme) were recorded at 1-min intervals following addition of 1 mM NADH. (B) As for panel A, except miconazole (13 μM) was added prior to the addition of NADH. Arrows indicate the direction of the absorbance change. (C) Time course for NADH-mediated reduction of flavoHb-Fe(III) (line 1) and flavoHb-Fe(III)-miconazole complex (line 2) as measured by the absorbance changes at 433 nm and 427 nm, respectively. (D) Time course for reduction of FAD in flavoHb-FAD/Fe(III) (line 1) and flavoHb-FAD/Fe(III)-miconazole (line 2) measured at 460 nm. DMSO was present at a final concentration of 1.3% (vol/vol).

complex when compared to that of the ferric enzyme (Fig. 4C, compare lines 1 and 2). The estimated first-order rate constant for ferric heme reduction by NADH (k_{ET}) decreased from ~150 s^{-1} for the miconazole-free reaction (19) to <0.004 s^{-1} for the miconazole complex. Coordination of miconazole to the heme iron also decreased the rate of FAD reduction as measured by the change in absorbance at 460 nm (Fig. 4D). The lower rate of FAD reduction may be explained by an allosteric effect of imidazole binding in the distal pocket on the NADH-FAD electron transfer reaction and a lower rate constant for hydride transfer (k'_H). Similar effects on heme and FAD reduction were observed with econazole, clotrimazole, and ketoconazole (data not shown).

Imidazoles inhibit NO metabolism in microbes. In *S. cerevisiae*, *C. albicans*, and *E. coli*, >95% of the aerobic NO metabolic activity is catalyzed by the flavoHbs (25, 55). Imidazoles were investigated for their ability to inhibit NO metabolism by intact cells. In *S. cerevisiae*, miconazole showed 50% inhibition

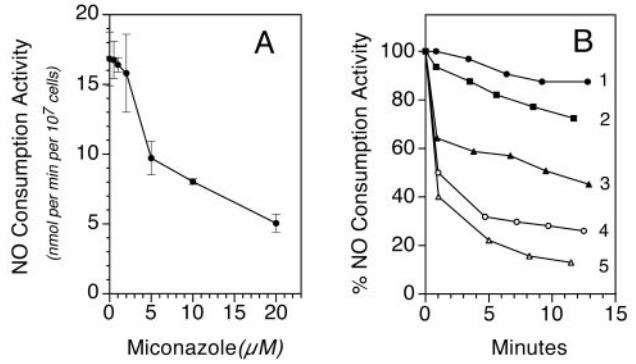

FIG. 5. Effect of miconazole on NO metabolism in *S. cerevisiae*. (A) NO consumption by *S. cerevisiae* was assayed with various concentrations of miconazole. (B) Time dependence of activity loss in the presence of 0, 2, 5, 10, or 50 μM miconazole as indicated (lines 1–5). DMSO was added as the solvent to a final concentration of 0.1% (vol/vol). Error bars represent standard deviations of the average for three independent trials.

of NO metabolism at 10 μM (Fig. 5A). Inhibition was rapid and progressive (Fig. 5B), suggesting efficient uptake and accumulation within cells. Similar effects of miconazole were observed in *C. albicans*. Treatment of *Candida* with 0.5, 1, 2, 5, and 10 μM miconazole inhibited the inducible NOD activity (YHB1) (55) by 33, 51, 55, 68, and 84%, respectively. The greater sensitivity of the *C. albicans* NOD activity correlated with the lower K_i value determined for the purified enzyme (Table 1).

Although the purified *E. coli* NOD activity was more sensitive to miconazole (K_i = 80 nM) than either the *C. albicans* or *S. cerevisiae* enzymes, NO consumption by *E. coli* was only modestly inhibited by miconazole and other imidazoles. *E. coli* expressing a level of NOD activity of 116 ± 12 nmol NO/min/10^8 cells was inhibited by 34 ± 5, 41 ± 3, and 24 ± 3% following incubation with 50 μM miconazole, econazole, and clotrimazole, respectively. The results are consistent with the poor membrane permeability and antibiotic activity of imidazoles toward gram-negative *E. coli* (3, 48). By comparison, NO metabolism in gram-positive *S. aureus* was more sensitive to imidazole inhibition. *S. aureus* expressing a basal NOD activity of 2.6 ± 0.6 (n = 3) nmol NO/min/10^8 cells and an induced level of activity of 6.5 ± 0.2 nmol NO/min/10^8 cells (n = 3) following a 120-min exposure to 960 ppm NO was rapidly inhibited by imidazoles. Miconazole, econazole, or clotrimazole (5 μM) inhibited the induced NO metabolic activity by 92% ± 3%, 68% ± 3%, and 41% ± 3%, respectively.

Effects of NO and imidazoles on *S. cerevisiae and C. albicans* growth. We tested the sensitivity of *S. cerevisiae* to miconazole with and without exposure to NO during aerobic growth in nutrient-rich YPD medium. As shown in Fig. 6A, 5 μM miconazole caused modest growth inhibition under these conditions (compare lines 1 and 3) while 960 ppm NO (≤2 μM in solution) showed negligible effects on growth (compare lines 1 and 2). However, simultaneous exposure of yeasts to miconazole and NO strongly inhibited growth (line 4). The doubling time increased from 180 min for miconazole treatment alone to ~720 min for miconazole and NO. By comparison, the doubling time increased from 90 to ~300 min following expo-

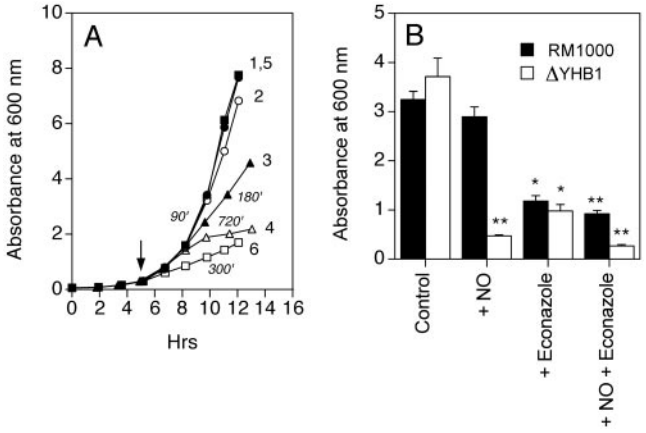

FIG. 6. Effect of NO and imidazoles on *S. cerevisiae* and *C. albicans* growth. (A) Cultures of *S. cerevisiae* strain BY4742 (lines 1–4) and the isogenic NOD-deficient mutant *yhb1*Δ (lines 5 and 6) were grown under a normoxic atmosphere in the absence (lines 1, 3, and 5) or presence of 960 ppm NO gas (lines 2, 4, and 6). Miconazole (lines 3 and 4) (5 μM) and NO were delivered at the time indicated by the arrow. Approximate generation times (minutes) are given in italics. (B) Cultures of *C. albicans* strain RM1000 and the isogenic NOD-deficient mutant *yhb1*Δ/*yhb1*Δ (ΔYHB1) were grown in modified YPD medium containing 5 mM glucose and 10 μM O_2. Cultures were exposed to 160 ppm NO (<0.3 μM in solution) with or without 5 μM econazole. After 20 h, growth was measured by the absorbance at 600 nm. Single asterisks indicate a P of <0.05 relative to the control condition. Double asterisks indicate a P of <0.05 relative to both the control condition and between strains.

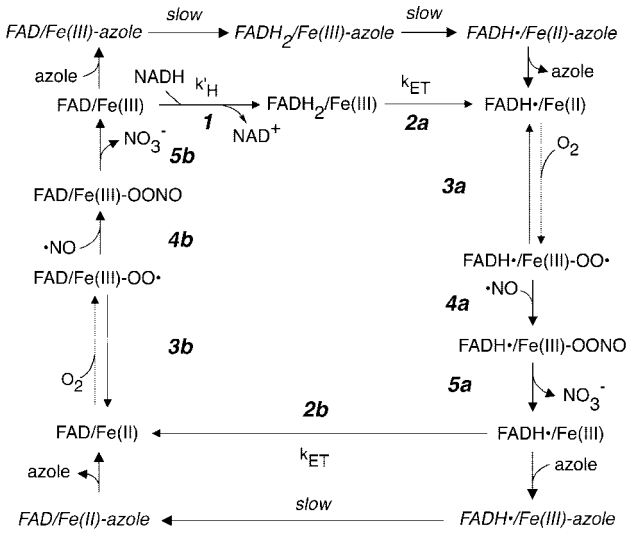

FIG. 7. Proposed mechanism for imidazole inhibition of NOD. Azoles coordinate the ferric heme iron and impair hydride transfer (k'_H) (step 1) and electron transfer (k_{ET}) (steps 2a and 2b). Azoles readily dissociate from the reduced ferrous heme iron, allowing O_2 binding and formation of Fe(III)-O_2 · (steps 3a and 3b). Rapid reaction of · NO with the Fe(III)-O_2 · intermediate forms the ferric-peroxynitrite intermediate (4a and 4b), which rapidly isomerizes to produce nitrate and flavoHb-Fe(III) (5a and 5b).

sure of the NOD-deficient mutant (*yhb1*Δ) to NO (compare lines 5 and 6), revealing the potential contribution of NOD inhibition to growth stasis. Together, the results in Fig. 5 and 6A support an antibiotic mechanism for miconazole involving NOD inhibition. Nevertheless, at these relatively high miconazole concentrations, the increased NO sensitivity of *S. cerevisiae* could also be due in part to miconazole impairment of membrane synthesis, membrane integrity, and other cell functions (1, 30, 53, 58).

Under conditions mimicking microaerobic *C. albicans* infection, 160 ppm NO gas exposure (<0.3 μM in solution) also showed strong inhibition of the growth of the NOD-deficient *C. albicans* mutant (ΔYHB1) but not the isogenic parental strain RM1000 (Fig. 6B, compare open and solid bars). Unlike the effect of miconazole on the NO sensitivity of *S. cerevisiae*, econazole (5 μM) did not increase the sensitivity of strain RM1000 to NO. The results suggest that econazole accumulates in *C. albicans* at levels that are too low to effectively inhibit NOD (K_i = 225 nM) but at concentrations sufficient to inhibit the sensitive lanosterol 14α-demethylase (58).

DISCUSSION

Mechanism of NOD inhibition. FlavoHb-type NODs possess remarkably large hydrophobic heme pockets capable of sequestering bulky aliphatic lipids (28, 44) and imidazole N-1 substituents. Indeed, the ability of large hydrophobic imidazoles (58) to inhibit NODs correlates remarkably well with the affinity of heme pockets for lipids: *A. eutrophus* > *E. coli* > *S. cerevisiae* (Table 1) (44). Furthermore, the ability of a single chlorine atom of miconazole to confer a 2.5- to 20-fold decrease in the K_i value from that for econazole suggests specific interactions with the large hydrophobic N-1 substituent affecting the geometric orientation and subsequent coordination to heme iron. An exception is the *C. albicans* NOD, which exhibits an ~3-fold greater sensitivity to econazole than to miconazole (Table 1). The lower sensitivity of the *S. cerevisiae* NOD to imidazoles in general suggests weaker interactions between the N-1 substituents and the distal hydrophobic pocket. Alternatively, certain flavoHb structures may control entry of N-1-substituted imidazoles into the heme pocket, as suggested by structural studies of the *M. tuberculosis* 14α-sterol demethylase (product of *CYP51*) (47). Our kinetic and spectral results suggest a mechanism for NOD inhibition involving high affinity binding of imidazoles to the flavoHb-Fe(III) intermediate (Fig. 7) (20). Thus, uncompetitive inhibition by imidazoles, with respect to O_2 (Fig. 2A), reveals a mechanism of inhibition largely independent of O_2 and flavoHb-Fe(II). In contrast, CO competitively inhibits NOD with respect to O_2 by forming a high-affinity flavoHb-Fe(II) CO complex (24). The failure of imidazoles to compete with NO (Fig. 2B) also rules out mechanisms involving interference with the NO dioxygenation reaction (Fig. 7, reaction steps 4a and 4b). Furthermore, increased inhibition by NO in the presence of miconazole (Fig. 2B) suggests a secondary mechanism involving increased accessibility of NO for flavoHb-Fe(II) (19). The apparent K_i values for imidazoles (Table 1) presumably reflect composite equilibrium dissociation constants with the affinity of imidazoles for flavoHb-Fe(III) being far greater than for flavoHb-Fe(II) (Fig. 7). Together, the results support a mechanism in which imidazole binding to the flavoHb-Fe(III) intermediate impairs the reduction of heme and FAD (Fig. 7, reaction steps

1, 2a, and 2b), thus limiting subsequent steps in NOD turnover. Figure 7 also predicts greater imidazole inhibition with decreased NADH availability or poor reductase coupling as reflected by a lower k_{ET}. It is noteworthy that imidazoles also show preference for ferric heme iron in lanosterol 14α-demethylase (63), suggesting similar mechanisms for inhibition.

Antibiotic action of imidazoles and NOD inhibition. Imidazoles and triazoles inhibit the heme-dependent lanosterol 14α-demethylase at low nanomolar concentrations and alter sterol synthesis and membrane biogenesis and stability in yeasts and fungi. Lanosterol 14α-demethylase inhibition is responsible for the antibiotic activity of these agents towards a variety of pathogenic yeast and fungi (33, 42, 57, 58, 62, 63). Azoles are widely used for treating various mycoses of skin, mucosa, and subcutaneous tissue. Ketoconazole, and more commonly itraconazole, and other potent triazole-based inhibitors of the lanosterol 14α-demethylase are administered for systemic fungal infections (5, 29, 42, 48, 52, 54, 58). In addition, antifungal imidazoles show antibacterial activity (5, 48, 49, 52, 56, 59), yet the antibiotic mechanisms remain to be fully elucidated.

Our results demonstrate that the NOD function of yeast, fungal, and bacterial flavoHbs can also be inhibited by antifungal imidazoles, albeit at greater than 100-fold higher concentrations than reported for the fungal and yeast lanosterol 14α-demethylase (33, 57, 58). Imidazoles coordinated heme and inhibited NOD activity of the purified bacterial, yeast, and fungal flavoHbs (Table 1). Imidazoles also inhibited NOD activities in *S. cerevisiae* (Fig. 5), *C. albicans*, and *S. aureus* and to a much lesser extent within *E. coli*. Moreover, miconazole increased NO-mediated growth inhibition of *S. cerevisiae* (Fig. 6A). On the other hand, the results do not exclude a mechanism involving NO sensitization due to lanosterol 14α-demethylase inhibition as previously suggested for clotrimazole sensitization of *C. albicans* to hydrogen peroxide (50) or the direct inhibition of membrane-bound ATPases and cytochrome oxidase, as well as the synthesis of mitochondrial and peroxisomal enzymes including peroxidase and catalase (8, 9, 30). Indeed, antibiotic synergy between imidazoles and NO-releasing diazeniumdiolates was previously reported for *Candida* (34) and may also be explained by NOD-independent mechanisms since the agents inhibited NOD weakly. Furthermore, the expression of inducible pumps for imidazole removal (58, 60) coupled with relatively high K_i values (Table 1) may preclude econazole and other imidazoles from effectively inhibiting NOD activity in *C. albicans* and other organisms.

Nevertheless, the potency of NO as an antibiotic in the absence of NOD (Fig. 6) (20) and the sensitivity of NODs to imidazoles (Table 1) encourage the search for imidazoles that more effectively inhibit NOD function. Knowledge of flavoHb-Fe(III)-imidazole structures and the availability of a rich pharmacopoeia of imidazoles and triazoles for testing should facilitate the identification and design of more efficacious NOD inhibitors. The unique sensitivity of the bacterial NODs to miconazole also motivates investigations of synergy between NO, miconazole, and antibacterial agents such as polymyxin B that can increase the penetration of miconazole through *E. coli* membranes (3).

ACKNOWLEDGMENTS

We thank John Olson and Melanie Cushion for comments and discussion.

This work was supported in part by a Public Health Service Grant (R01 GM65090) from the Institute of General Medical Sciences to P.R.G. and a National Science Foundation Grant (MCB 0091236) to M.C.G. R.A.H. was supported by an Underrepresented Minority Training Supplement to R01 GM65090. A.N.H. was supported by a Public Health Service Training Grant (T32 GM008280) to the Houston Area Molecular Biophysics Program from the Institute of General Medical Sciences.

REFERENCES

1. **Bammert, G. F., and J. M. Fostel.** 2000. Genome-wide expression patterns in *Saccharomyces cerevisiae*: comparison of drug treatments and genetic alterations affecting biosynthesis of ergosterol. Antimicrob. Agents Chemother. **44:**1255–1265.
2. **Bellamine, A., A. T. Mangla, W. D. Nes, and M. R. Waterman.** 1999. Characterization and catalytic properties of the sterol 14α-demethylase from *Mycobacterium tuberculosis*. Proc. Natl. Acad. Sci. USA **96:**8937–8942.
3. **Cornelissen, F., and H. Van den Bossche.** 1983. Synergism of the antimicrobial agents miconazole, bactracin and polymyxin B. Chemotherapy **29:**419–427.
4. **Crawford, M. J., and D. E. Goldberg.** 1998. Regulation of the *Salmonella typhimurium* flavohemoglobin gene. A new pathway for bacterial gene expression in response to nitric oxide. J. Biol. Chem. **273:**34028–34032.
5. **Dabbs, E. R., S. Naidoo, C. Lephoto, and N. Nikitina.** 2003. Pathogenic *Nocardia*, *Rhodococcus*, and related organisms are highly susceptible to imidazole antifungals. Antimicrob. Agents Chemother. **47:**1476–1478.
6. **De Backer, M. D., T. Ilyina, X.-J. Ma, S. Vandoninck, W. H. M. L. Luyten, and H. Vanden Bossche.** 2001. Genomic profiling of the response of *Candida albicans* to itraconazole treatment using DNA microarray. Antimicrob. Agents Chemother. **45:**1660–1670.
7. **de Jesús-Berrîos, M., L. Liu, J. C. Nussbaum, G. M. Cox, J. S. Stamler, and J. Heitman.** 2003. Enzymes that counteract nitrosative stress promote fungal virulence. Curr. Biol. **13:**1963–1968.
8. **De Nollin, S., and M. Borgers.** 1977. The effects of miconazole on the ultrastructure of *Candida albicans*. Proc. R. Soc. Med. **70:**9–12.
9. **De Nollin, S., H. Van Belle, F. Goossens, F. Thone, and M. Borgers.** 1977. Cytochemical and biochemical studies of yeasts after in vitro exposure to miconazole. Antimicrob. Agents Chemother. **11:**500–513.
10. **Eriksson, S., S. Lucchini, A. Thompson, M. Rhen, and J. C. D. Hinton.** 2003. Unravelling the biology of macrophage infection by gene expression profiling of intracellular *Salmonella enterica*. Mol. Microbiol. **47:**103–118.
11. **Ermler, U., R. A. Siddiqui, R. Cramm, and B. Friedrich.** 1995. Crystal structure of the flavohemoglobin from *Alcaligenes eutrophus* at 1.75Å resolution. EMBO J. **14:**6067–6077.
12. **Fang, F. C.** 2004. Antimicrobial reactive oxygen and nitrogen species: concepts and controversies. Nat. Rev. Microbiol. **2:**820–832.
13. **Favey, S., G. Labesse, V. Vouille, and M. Boccara.** 1995. Flavohaemoglobin HmpX: a new pathogenicity determinant in *Erwinia chrysanthemi* strain 3937. Microbiology **141:**863–871.
14. **Firoved, A. M., and V. Deretic.** 2003. Microarray analysis of global gene expression in mucoid *Pseudomonas aeruginosa*. J. Bacteriol. **185:**1071–1081.
15. **Frey, A. D., J. Farrés, C. J. T. Bollinger, and P. T. Kallio.** 2002. Bacterial hemoglobins and flavohemoglobins for alleviation of nitrosative stress in *Escherichia coli*. Appl. Environ. Microbiol. **68:**4835–4840.
16. **Gardner, A. M., and P. R. Gardner.** 2002. Flavohemoglobin detoxifies nitric oxide in aerobic, but not anaerobic, Escherichia coli: evidence for a novel inducible anaerobic nitric oxide scavenging activity. J. Biol. Chem. **277:**8166–8171.
17. **Gardner, A. M., C. R. Gessner, and P. R. Gardner.** 2003. Regulation of the nitric oxide reduction operon (*norRVW*) in Escherichia coli. Role of NorR and σ^{54} in the nitric oxide stress response. J. Biol. Chem. **278:**10081–10086.
18. **Gardner, A. M., R. A. Helmick, and P. R. Gardner.** 2002. Flavorubredoxin: an inducible catalyst for nitric oxide reduction and detoxification in *Escherichia coli*. J. Biol. Chem. **277:**8172–8177.
19. **Gardner, A. M., L. A. Martin, P. R. Gardner, Y. Dou, and J. S. Olson.** 2000. Steady-state and transient kinetics of *Escherichia coli* nitric oxide dioxygenase (flavohemoglobin): the tyrosine B10 hydroxyl is essential for dioxygen binding and catalysis. J. Biol. Chem. **275:**12581–12589.
20. **Gardner, P. R.** 2005. Nitric oxide dioxygenase function and mechanism of flavohemoglobin, hemoglobin, myoglobin and their associated reductases. J. Inorg. Biochem. **99:**247–266.
21. **Gardner, P. R., G. Costantino, and A. L. Salzman.** 1998. Constitutive and adaptive detoxification of nitric oxide in *Escherichia coli*. Role of nitric oxide dioxygenase in the protection of aconitase. J. Biol. Chem. **273:**26528–26533.
22. **Gardner, P. R., G. Costantino, C. Szabó, and A. L. Salzman.** 1997. Nitric oxide sensitivity of the aconitases. J. Biol. Chem. **272:**25071–25076.
23. **Gardner, P. R., A. M. Gardner, and C. K. Hallstrom.** 2004. Dioxygen-

dependent metabolism of nitric oxide, p. 133–150. *In* A. Hassid (ed.), Nitric oxide protocols, 2nd ed., vol. 279. Humana Press, Totowa, N.J.
24. **Gardner, P. R., A. M. Gardner, L. A. Martin, Y. Dou, T. Li, J. S. Olson, H. Zhu, and A. F. Riggs.** 2000. Nitric oxide dioxygenase activity and function of flavohemoglobins. Sensitivity to nitric oxide and carbon monoxide inhibition. J. Biol. Chem. **275:**31581–31587.
25. **Gardner, P. R., A. M. Gardner, L. A. Martin, and A. L. Salzman.** 1998. Nitric oxide dioxygenase: an enzymic function for flavohemoglobin. Proc. Natl. Acad. Sci. USA **95:**10378–10383.
26. **Hausladen, A., A. J. Gow, and J. S. Stamler.** 1998. Nitrosative stress: metabolic pathway involving the flavohemoglobin. Proc. Natl. Acad. Sci. USA **95:**14100–14105.
27. **Hibbs, J. B., Jr.** 2002. Infection and nitric oxide. J. Infect. Dis. **185:**S9–S17.
28. **Ilari, A., A. Bonamore, A. Farina, K. A. Johnson, and A. Boffi.** 2002. The X-ray structure of ferric *Escherichia coli* flavohemoglobin reveals an unexpected geometry of the distal heme pocket. J. Biol. Chem. **277:**23725–23732.
29. **Jones, B. M., I. Geary, M. E. Lee, and B. I. Duerden.** 1989. Comparison of the in vitro activities of fenticonazole, other imidazoles, metronidazole, and tetracycline against organisms associated with bacterial vaginosis and skin infections. Antimicrob. Agents Chemother. **33:**970–972.
30. **Kerridge, D.** 1986. Mode of action of clinically important antifungal drugs. Adv. Microb. Physiol. **27:**1–72.
31. **Liu, L., M. Zeng, A. Hausladen, J. Heitman, and J. S. Stamler.** 2000. Protection from nitrosative stress by yeast flavohemoglobin. Proc. Natl. Acad. Sci. USA **97:**4672–4676.
32. **Lowry, O. H., N. J. Rosebrough, A. L. Farr, and R. J. Randall.** 1951. Protein measurement with the Folin phenol reagent. J. Biol. Chem. **193:**265–275.
33. **Marriott, M. S.** 1980. Inhibition of sterol biosynthesis in *Candida albicans* by imidazole-containing antifungals. J. Gen. Microbiol. **117:**253–255.
34. **McElhaney-Feser, G. E., R. E. Raulli, and R. L. Cihlar.** 1998. Synergy of nitric oxide and azoles against *Candida* species in vitro. Antimicrob. Agents Chemother. **42:**2342–2346.
35. **McLean, K. J., M. R. Cheesman, S. L. Rivers, A. Richmond, D. Leys, S. K. Chapman, G. A. Reid, N. C. Price, S. M. Kelly, J. Clarkson, W. E. Smith, and A. W. Munro.** 2002. Expression, purification and spectroscopic characterization of the P450 CYP121 from *Mycobacterium tuberculosis*. J. Inorg. Biochem. **91:**527–541.
36. **Membrillo-Hernández, J., M. D. Coopamah, M. F. Anjum, T. M. Stevanin, A. Kelly, M. N. Hughes, and R. K. Poole.** 1999. The flavohemoglobin of *Escherichia coli* confers resistance to a nitrosating agent, a "nitric oxide releaser," and paraquat and is essential for transcriptional responses to oxidative stress. J. Biol. Chem. **274:**748–754.
37. **Moore, C. M., M. M. Nakano, T. Wang, R. W. Ye, and J. D. Helmann.** 2004. Response of *Bacillus subtilis* to nitric oxide and the nitrosating agent sodium nitroprusside. J. Bacteriol. **186:**4655–4664.
38. **Mukhopadhyay, P., M. Zheng, L. A. Bedzyk, R. A. LaRossa, and G. Storz.** 2004. Prominent roles of the NorR and Fur regulators in the *Escherichia coli* transcriptional response to reactive nitrogen species. Proc. Natl. Acad. Sci. USA **101:**745–750.
39. **Nakahara, K., T. Tanimoto, K.-I. Hatano, K. Usuda, and H. Shoun.** 1993. Cytochrome P-450 55A1 (P-450dNIR) acts as nitric oxide reductase employing NADH as the direct electron donor. J. Biol. Chem. **268:**8350–8355.
40. **Nathan, C.** 2004. Antibiotics at the crossroads. Are we making the right choices to bring new drugs to the marketplace? Nature **431:**899–902.
41. **Nathan, C.** 1992. Nitric oxide as a secretory product of mammalian cells. FASEB J. **6:**3051–3064.
42. **Nicholas, R. O., and D. Kerridge.** 1989. Correlation of inhibition of sterol synthesis with growth-inhibitory action of imidazole antimycotics in *Candida albicans*. J. Antimicrob. Chemother. **23:**7–19.
43. **Nozaki, Y.** 1986. Determination of the concentration of protein by dry weight—a comparison with spectrophotometric methods. Arch. Biochem. Biophys. **249:**437–446.
44. **Ollesch, G., A. Kaunzinger, D. Juchelka, M. Schubert-Zsilavecz, and U. Ermler.** 1999. Phospholipid bound to the flavohemoprotein from *Alcaligenes eutrophus*. Eur. J. Biochem. **262:**396–405.
45. **Ouellet, H., Y. Ouellet, C. Richard, M. Labarre, B. Wittenberg, J. Wittenberg, and M. Guertin.** 2002. Truncated hemoglobin HbN protects *Mycobacterium bovis* from nitric oxide. Proc. Natl. Acad. Sci. USA **99:**5902–5907.
46. **Pathania, R., N. K. Navani, A. M. Gardner, P. R. Gardner, and K. L. Dikshit.** 2002. Nitric oxide scavenging and detoxification by the *Mycobacterium tuberculosis* haemoglobin, HbN in *Escherischia coli*. Mol. Microbiol. **45:**1303–1314.
47. **Podust, L. M., T. L. Poulos, and M. R. Waterman.** 2001. Crystal structure of cytochrome P450 14α-sterol demethylase (CYP51) from *Mycobacterium tuberculosis* in complex with azole inhibitors. Proc. Natl. Acad. Sci. USA **98:**3068–3073.
48. **Schär, G., F. H. Kayser, and M. C. Dupont.** 1976. Antimicrobial activity of econazole and miconazole *in vitro* and in experimental candidiasis and aspergillosis. Chemotherapy **22:**211–220.
49. **Schierholz, J. M., C. Fleck, J. Beuth, and G. Pulverer.** 2000. The antimicrobial efficacy of a new central venous catheter with long-term broad-spectrum activity. J. Antimicrob. Chemother. **46:**45–50.
50. **Shimokawa, O., and K. Nakayama.** 1992. Increased sensitivity of *Candida albicans* cells accumulating 14α-methylated sterols to active oxygen: possible relevance to in vivo efficacies of azole antifungal agents. Antimicrob. Agents Chemother. **36:**1626–1629.
51. **Stevanin, T. M., R. K. Poole, E. A. G. Demoncheaux, and R. C. Read.** 2002. Flavohemoglobin Hmp protects *Salmonella enterica* serovar Typhimurium from nitric oxide-related killing by human macrophages. Infect. Immun. **70:**4399–4405.
52. **Sud, I. J., and D. S. Feingold.** 1982. Action of antifungal imidazoles on *Staphylococcus aureus*. Antimicrob. Agents Chemother. **22:**470–474.
53. **Sud, I. J., and D. S. Feingold.** 1981. Heterogeneity of action mechanisms among antimycotic imidazoles. Antimicrob. Agents Chemother. **20:**71–74.
54. **Sun, Z., and Y. Zhang.** 1999. Antituberculosis activity of certain antifungal and antihelmintic drugs. Tuber. Lung Dis. **79:**319–320.
55. **Ullmann, B. D., H. Myers, W. Chiranand, A. L. Lazzell, Q. Zhao, L. A. Vega, J. L. Lopez-Ribot, P. R. Gardner, and M. C. Gustin.** 2004. An inducible defense mechanism against nitric oxide in *Candida albicans*. Eukaryot. Cell **3:**715–723.
56. **Vanden Bossche, H., F. Cornelissen, and J. Van Cutsem.** 1982. Synergism of the antimicrobial agents miconazole and benzoylperoxide. Br. J. Dermatol. **107:**343–348.
57. **Van den Bossche, H., G. Willemsens, W. Cools, W. F. J. Lauwers, and L. Le Jeune.** 1978. Biochemical effects of miconazole on fungi. II. Inhibition of ergosterol biosynthesis in *Candida albicans*. Chem. Biol. Interact. **21:**59–78.
58. **Vanden Bossche, H., M. Engelen, and F. Rochette.** 2003. Antifungal agents of use in animal health-chemical, biochemical and pharmacological aspects. J. Vet. Pharmacol. Ther. **26:**5–29.
59. **von Recklinghausen, G., C. Di Maio, and R. Ansorg.** 1993. Activity of antibiotics and azole antimycotics against *Helicobacter pylori*. Zentralbl. Bakteriol. **280:**279–285.
60. **White, T. C., K. A. Marr, and R. A. Bowden.** 1998. Clinical, cellular, and molecular factors that contribute to antifungal drug resistance. Clin. Microbiol. Rev. **11:**382–402.
61. **Yanisch-Perron, C., C. Vieira, and J. Messing.** 1985. Improved M13 phage cloning vectors and host strains: nucleotide sequences of the M13mp18 and pUC19 vectors. Gene **33:**103–119.
62. **Yoshida, Y.** 1988. Cytochrome P450 of fungi: primary target for azole antifungal agents. Curr. Top. Med. Mycol. **2:**388–418.
63. **Yoshida, Y., and Y. Aoyama.** 1987. Interaction of azole antifungal agents with cytochrome $P\text{-}450_{14DM}$ purified from *Saccharomyces cerevisiae* microsomes. Biochem. Pharmacol. **36:**229–235.
64. **Zumft, W.** 1997. Cell biology and molecular basis of denitrification. Microbiol. Mol. Biol. Rev. **61:**533–616.